

# METTL1/WDR4-mediated m<sup>7</sup>G tRNA modifications and m<sup>7</sup>G codon usage promote mRNA translation and lung cancer progression

Jieyi Ma,<sup>1,2,7</sup> Hui Han,<sup>2,7</sup> Ying Huang,<sup>3,7</sup> Chunlong Yang,<sup>2</sup> Siyi Zheng,<sup>2</sup> Tiancai Cai,<sup>4</sup> Jiong Bi,<sup>1</sup> Xiaohui Huang,<sup>1</sup> Ruiming Liu,<sup>1</sup> Libin Huang,<sup>3</sup> Yifeng Luo,<sup>5</sup> Wen Li,<sup>1</sup> and Shuibin Lin<sup>2,6</sup>

<sup>1</sup>Laboratory of General Surgery, The First Affiliated Hospital, Sun Yat-sen University, Guangzhou 510080, China; <sup>2</sup>Center for Translational Medicine, Institute of Precision Medicine, The First Affiliated Hospital, Sun Yat-sen University, Guangzhou 510080, China; <sup>3</sup>Department of Pediatrics, The First Affiliated Hospital, Sun Yat-sen University, Guangzhou 510080, China; <sup>4</sup>Xiamen Special Service Convalescent Center, Xiamen 361005, China; <sup>5</sup>Department of Pulmonary and Critical Care Medicine, The First Affiliated Hospital of Sun Yat-sen University, Guangzhou 510080, China; <sup>6</sup>State Key Laboratory of Oncology in South China, Sun Yat-sen University Cancer Center, Guangzhou 510060, China

**Mis-regulated epigenetic modifications in RNAs are associated with human cancers. The transfer RNAs (tRNAs) are the most heavily modified RNA species in cells; however, little is known about the functions of tRNA modifications in cancers. In this study, we uncovered that the expression levels of tRNA N<sup>7</sup>-methylguanosine (m<sup>7</sup>G) methyltransferase complex components methyltransferase-like 1 (METTL1) and WD repeat domain 4 (WDR4) are significantly elevated in human lung cancer samples and negatively associated with patient prognosis. Impaired m<sup>7</sup>G tRNA modification upon METTL1/WDR4 depletion resulted in decreased cell proliferation, colony formation, cell invasion, and impaired tumorigenic capacities of lung cancer cells *in vitro* and *in vivo*. Moreover, gain-of-function and mutagenesis experiments revealed that METTL1 promoted lung cancer growth and invasion through regulation of m<sup>7</sup>G tRNA modifications. Profiling of tRNA methylation and mRNA translation revealed that highly translated mRNAs have higher frequencies of m<sup>7</sup>G tRNA-decoded codons, and knockdown of METTL1 resulted in decreased translation of mRNAs with higher frequencies of m<sup>7</sup>G tRNA codons, suggesting that tRNA modifications and codon usage play an essential function in mRNA translation regulation. Our data uncovered novel insights on mRNA translation regulation through tRNA modifications and the corresponding mRNA codon compositions in lung cancer, providing a new molecular basis underlying lung cancer progression.**

## INTRODUCTION

Lung cancer is one of the most common cancers and a leading cause of cancer-related death worldwide.<sup>1</sup> Genetic mutations, mis-regulated epigenetic modifications such as DNA methylation, chromatin organization, and histone modifications, play important roles in lung cancer progression.<sup>2</sup> However, the mechanisms underlying lung cancer oncogenesis are complicated and still not fully understood. Therefore, uncovering novel molecular mechanisms regulating lung cancer pro-

gression is essential for the development of new therapeutic strategies for effective lung cancer treatment.

Recent studies reveal the critical role of mRNA translation regulation in gene expression and disease progression.<sup>3</sup> Transfer RNAs (tRNAs) are adaptors in the protein translation machinery and contain various modifications, which are crucial for appropriate tRNA structure, stability, and function.<sup>4–8</sup> Currently, growing evidence reveals that the dysregulations of tRNA and its modifications catalyzing enzymes are involved in a variety of human diseases including cancers.<sup>9,10</sup> For example, global tRNA overexpression is found in breast cancer tissues and cells, which could favor the translation of cancer-related genes and thus promote cancer progression.<sup>11</sup> In addition, elevated expression of specific tRNAs can promote metastatic progression of breast cancer through regulating specific transcript stability and translation in a codon-specific modulation manner.<sup>12</sup> Moreover, deregulations of tRNA modification enzymes such as human tRNA methyltransferase 9-like (hTRM9L) and histone H2A dioxygenase ALKB homolog 1 (ALKBH1) caused impaired translation regulation and aberrant cancer progression *in vitro* and *in vivo*.<sup>13,14</sup> These studies demonstrate that aberrant tRNA expression level and tRNA modifications can result in cancer progression via disrupting

Received 8 November 2020; accepted 20 July 2021;  
<https://doi.org/10.1016/j.ymthe.2021.08.005>.

<sup>7</sup>These authors contributed equally

**Correspondence:** Yifeng Luo, Department of Pulmonary and Critical Care Medicine, The First Affiliated Hospital of Sun Yat-sen University, Guangzhou 510080, China.

**E-mail:** [lyif@mail.sysu.edu.cn](mailto:lyif@mail.sysu.edu.cn)

**Correspondence:** Wen Li, Laboratory of General Surgery, The First Affiliated Hospital, Sun Yat-sen University, Guangzhou 510080, China.

**E-mail:** [liwen@mail.sysu.edu.cn](mailto:liwen@mail.sysu.edu.cn)

**Correspondence:** Shuibin Lin, Center for Translational Medicine, Institute of Precision Medicine, The First Affiliated Hospital, Sun Yat-sen University, Guangzhou 510080, China.

**E-mail:** [linshb6@mail.sysu.edu.cn](mailto:linshb6@mail.sysu.edu.cn)

translation and protein expression, providing profound insights into tRNA-mediated translation regulation and tumorigenesis.

The N<sup>7</sup>-methylguanosine (m<sup>7</sup>G) modification at position 46 in tRNAs is widely found in eukaryotes and prokaryotes.<sup>15–17</sup> METTL1 and WDR4 form a methyltransferase complex that catalyzes m<sup>7</sup>G modification in tRNAs in eukaryotes.<sup>15–17</sup> Disruptions of the METTL1 or METTL1/WDR4 complex are correlated with many diseases including microcephalic primordial dwarfism, Galloway-Mowat syndrome, and tumor cell chemoresistance.<sup>17–21</sup> Our previous studies demonstrated that METTL1/WDR4-mediated m<sup>7</sup>G tRNA methylation is critical for stem cell self-renewal and differentiation, providing molecular evidence underlying abnormal m<sup>7</sup>G tRNA modification in human developmental diseases.<sup>16,22</sup> Despite its functional importance in stem cell biology and development, the roles of METTL1 and its mediated m<sup>7</sup>G tRNA modification in lung cancer remain unknown.

In this study, we find that METTL1 and WDR4 are significantly up-regulated in lung cancer samples and promote lung cancer progression *in vitro* and *in vivo*. Mechanistically, METTL1- and WDR4-mediated tRNA m<sup>7</sup>G modification regulate the translation of mRNAs with m<sup>7</sup>G tRNA-decoded codon (m<sup>7</sup>G codon) usage. Our data uncover a clear link between METTL1-mediated m<sup>7</sup>G tRNA modification and lung cancer progression, providing new insights for the development of therapeutic strategies for efficient lung cancer treatment.

## RESULTS

### Upregulated METTL1 and WDR4 expression is associated with poor prognosis of lung cancer patients

To study the role of METTL1- and WDR4-mediated m<sup>7</sup>G tRNA modifications in regulation of lung cancer, we first analyzed the expression of METTL1 and WDR4 in lung cancers using the lung adenocarcinoma (LUAD) and lung squamous cell carcinoma (LUSC) datasets from the Cancer Genome Atlas (TCGA). As shown in Figures 1A–1D, the expression levels of both METTL1 and WDR4 mRNAs are significantly upregulated in lung cancer tissues, compared to normal lung tissues. Interestingly, the expression levels of METTL1 and WDR4 mRNAs are significantly co-related in lung cancers (Figures 1E and 1F), suggesting the functional interplay between METTL1 and WDR4. Moreover, high levels of METTL1 and WDR4 are associated with poor patient survival, indicating potential functions of METTL1 and WDR4 in regulation of lung cancer progression (Figures 1G and 1H). To further confirm these results, we analyzed METTL1 expression by immunohistochemistry (IHC) using a lung cancer tissue array. Based on the staining intensities, samples were divided into two groups: the low METTL1 expression group (immunoreactivity score [IRS] < 3) and the high METTL1 expression group (IRS ≥ 3). The representative cases of different groups were shown in Figure 1I. Our data further confirmed that METTL1 expression is significantly upregulated in lung cancer tissues (Figures 1J and 1K). Western blot analysis also verified that both METTL1 and WDR4 are upregulated in human lung cancer

specimens, compared to their peri-tumor normal tissues (Figures 1L–1N). Moreover, the m<sup>7</sup>G modification levels are correspondingly elevated in lung cancer tissues (Figures 1L and 1O). Overall, these results reveal that METTL1 and WDR4 expressions are significantly upregulated in lung cancer and associated with poor prognosis of lung cancer patients, suggesting the potential oncogenic role of METTL1/WDR4 and their mediated m<sup>7</sup>G tRNA modification in lung cancer.

### METTL1 inhibition suppresses lung cancer cell proliferation, migration, and invasion *in vitro*

To investigate the effect of METTL1 on lung cancer, we first knocked down METTL1 expression in A549 and H1299 cells using lentiviruses expressing short hairpin (sh)GFP (negative control [NC]), shMETTL1-1 (shM1-1), or shMETTL1-2 (shM1-2) (Figures 2A and 2B). Interestingly, we found that knockdown of METTL1 reduced the expression of WDR4 but not other methyltransferases including METTL3 and METTL5 (Figures 2A and 2B; Figure S1A), suggesting that METTL1 stabilizes its cofactor WDR4 in lung cancer cells. MTT (3-(4,5-dimethylthiazol-2-yl)-2,5-diphenyltetrazolium bromide) assay showed that knockdown of METTL1 inhibited lung cancer cell proliferation *in vitro* (Figures 2C and 2D). In addition, both A549 and H1299 cells with depleted METTL1 exhibited reduced colony-formation capacities compared to the control groups (Figures 2E and 2F). Cell-cycle analysis revealed that METTL1 knockdown induced an increased ratio of G0/G1-phase cells and decreased the ratio of G2/M-phase cells in lung cancer cells (Figures 2G and 2H). We further carried out wound-healing and invasion assays to evaluate the effect of METTL1 on lung cancer cell migration and metastasis and found that METTL1 knockdown delayed wound closure and suppressed invasive abilities of both A549 and H1299 lung cancer cells (Figures 2I–2L). Overall, these results reveal that METTL1 is essential for lung cancer cell growth, migration, and invasion abilities *in vitro*.

### Knockdown of WDR4 impairs lung cancer cell growth and invasion capacities *in vitro*

WDR4 is an important cofactor of METTL1 and is essential for m<sup>7</sup>G modification on tRNAs.<sup>16</sup> To further study the role of m<sup>7</sup>G tRNA modifications in lung cancer progression, we infected lung cancer cells with lentiviruses expressing shGFP, shWDR4-1, or shWDR4-2 (Figures 3A and 3B). Our data revealed that depletion of WDR4 decreases METTL1 expression, suggesting that WDR4 is essential for maintaining METTL1 protein level (Figures 3A and 3B), which is consistent with the finding in yeast.<sup>23</sup> We next subjected these cells to proliferation and colony-formation assays and found that WDR4 knockdown led to decreased proliferation and reduced colony-formation activities in lung cancer cells (Figures 3C–3F). In addition, wound-healing and invasion assays further showed that knockdown of WDR4 inhibited migration and invasion of lung cancer cells (Figures 3G–3J), confirming the oncogenic function of WDR4 in lung cancers. Taken together, these results demonstrated that METTL1 and WDR4 play an important function in regulation of lung cancer growth and invasion *in vitro*.

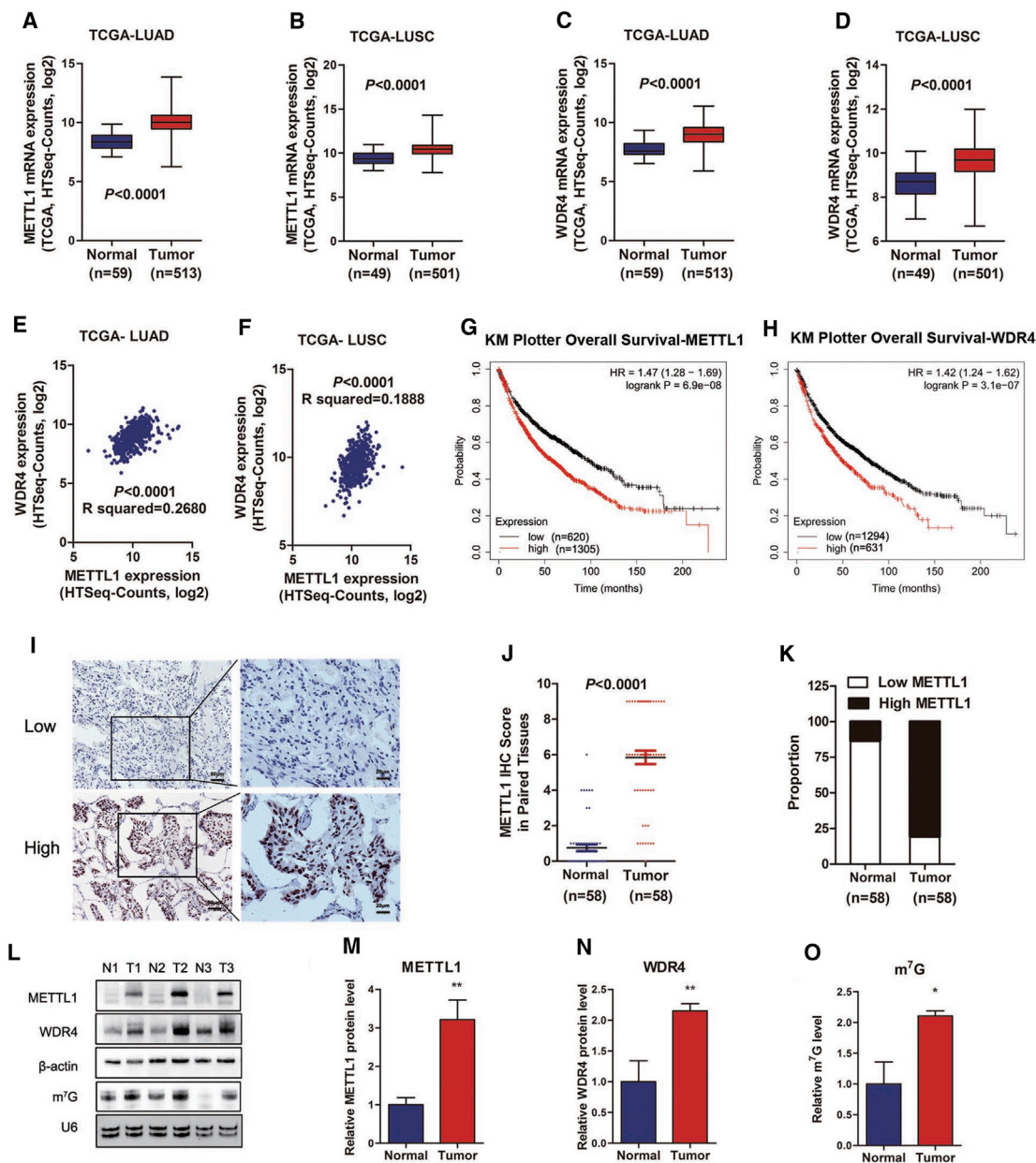


**Figure 1. Upregulated METTL1 and WDR4 expression in lung cancer samples**

(A and B) The expression level of METTL1 in normal tissues and lung cancer tissues from The Cancer Genome Atlas (TCGA) dataset. (C and D) The expression level of WDR4 in normal tissues and lung cancer tissues from TCGA dataset. (E and F) The expression levels of METTL1 and WDR4 in lung cancer were significantly co-related according to data from TCGA cohort. (G and H) Correlation between METTL1/WDR4 expression and overall survival of lung cancer patients according to the Kaplan-Meier Plotter database (<http://kmplot.com/analysis/>). (I) Representative IHC staining images of METTL1 in lung cancer tissues. Scale bars, 50  $\mu$ m and 20  $\mu$ m. (J) Quantitative IHC staining scores of METTL1 in 58 paired lung cancer tissues and normal tissues were shown. The expression of METTL1 was significantly increased in lung cancer specimens compared to adjacent non-tumor tissues. (K) Proportion of specimens according to METTL1 expression levels by IHC. (L) The expression level of METTL1 and WDR4 in human lung cancer tissues was detected by western blot assay, and m<sup>7</sup>G tRNA modification levels were examined by the northwestern blot.  $\beta$ -actin and U6 small nuclear RNA (snRNA) were used as loading control, respectively. (M–O) Quantitative analysis of METTL1 (M) and WDR4 (N) protein levels and m<sup>7</sup>G modification level (O). Data were presented as mean  $\pm$  SEM (Student's t test, \* $p < 0.05$ , \*\* $p < 0.01$ , \*\*\* $p < 0.001$ , compared to the normal tissues). LUAD, lung adenocarcinoma; LUSC, lung squamous cell carcinoma; N, normal lung tissue; T, tumor tissue.

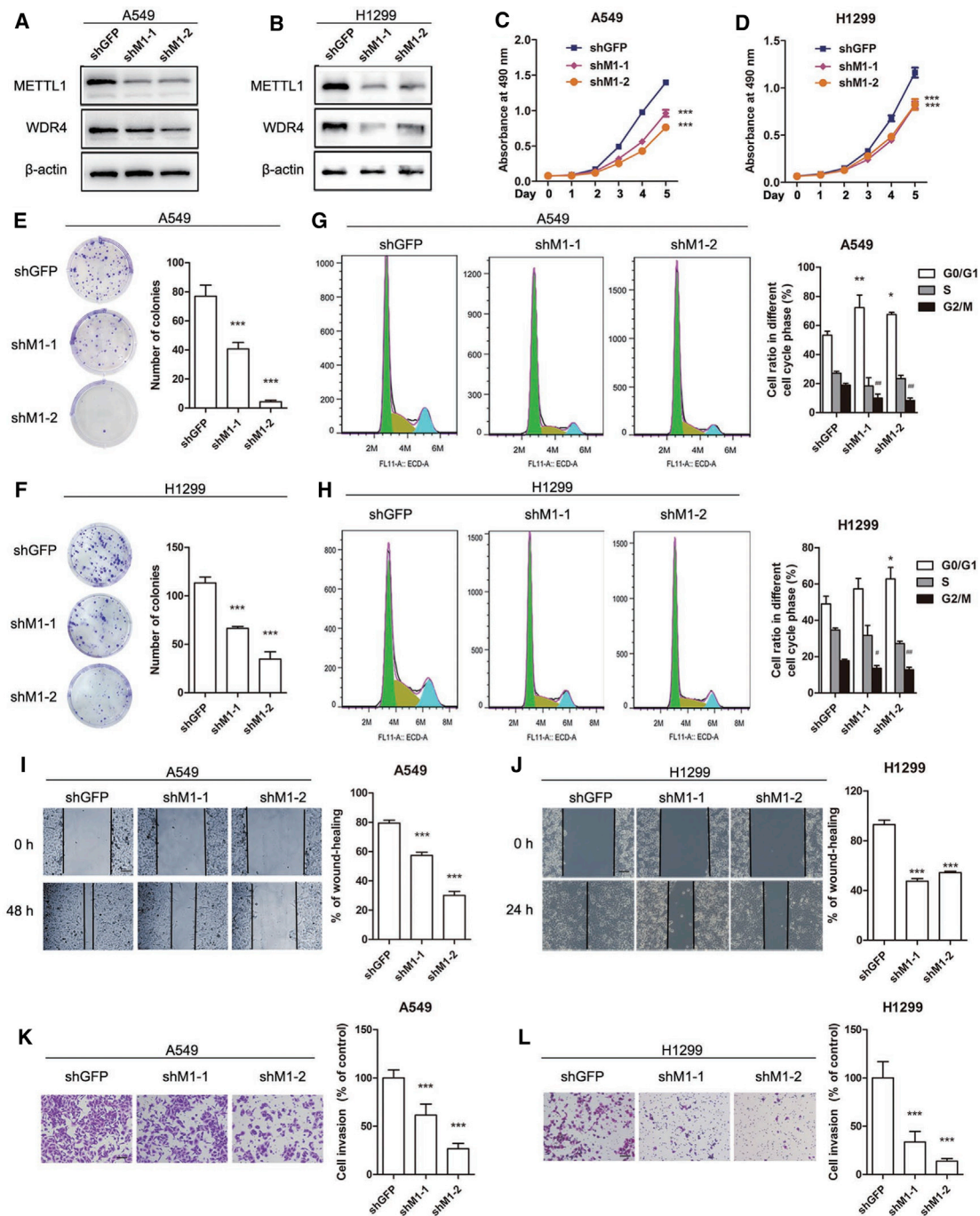


**Figure 2. Inhibition of METTL1 impairs lung cancer progression *in vitro***

(A and B) Validation of the depleted effect of short hairpin (sh)METTL1 by western blot in A549 and H1299 lung cancer cells. (C and D) Knockdown of METTL1 suppressed proliferation of A549 and H1299 cells. (E and F) METTL1-depleted A549 and H1299 lung cancer cells formed less colonies in colony-formation assays. (G and H) Knockdown of METTL1 induced an increased ratio of G0/G1-phase cells and decreased the ratio of G2/M-phase cells in lung cancer cells. (I–L) Knockdown of METTL1 suppressed cell migration (I and J) and invasion (K and L) in A549 and H1299 cells. Data were presented as mean  $\pm$  SD. Scale bar, 100  $\mu$ m. (One-way ANOVA, \* $p$  < 0.05, \*\* $p$  < 0.01, \*\*\* $p$  < 0.001, # $p$  < 0.05, ## $p$  < 0.01, compared to shGFP.)

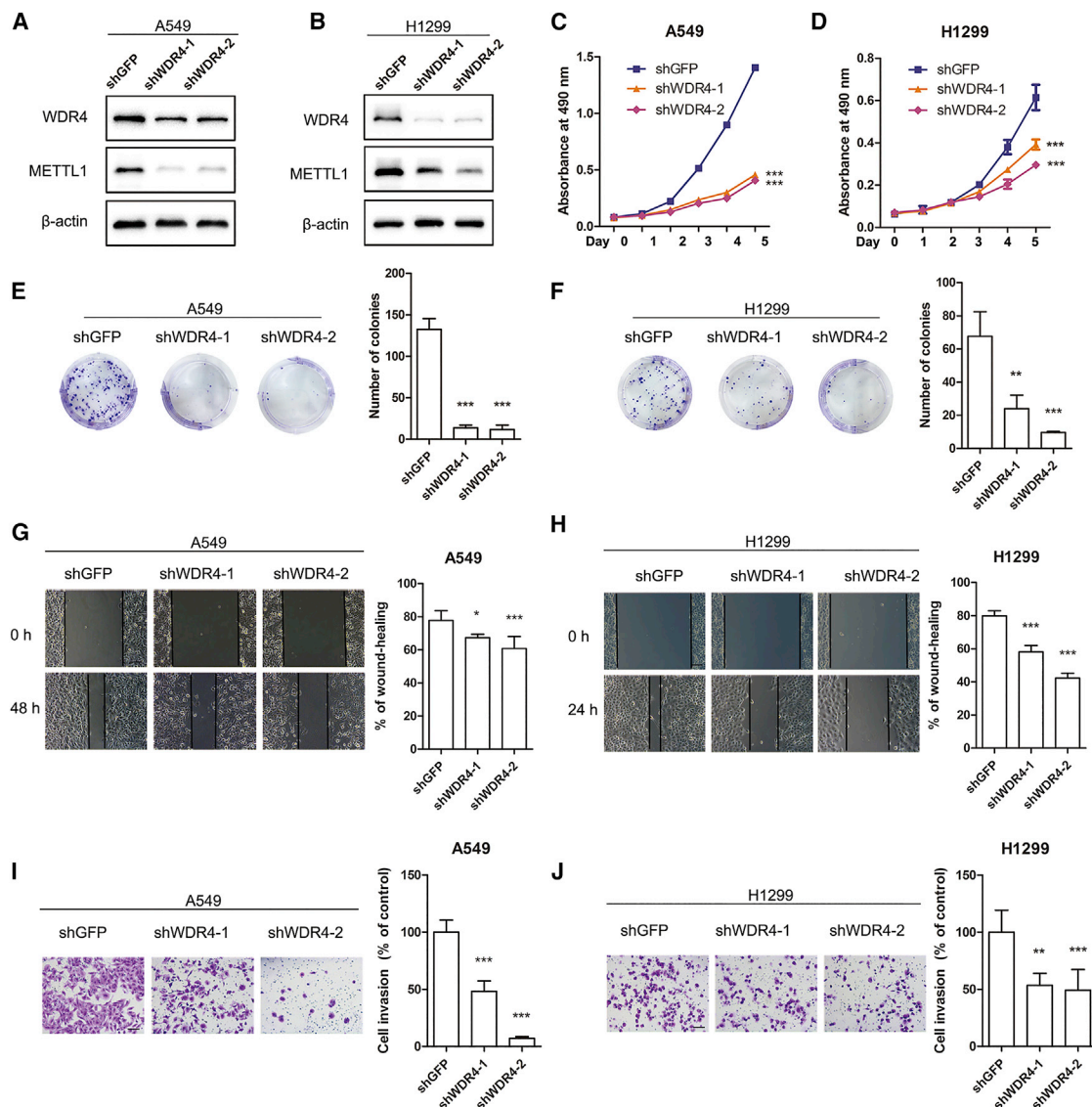


**Figure 3. WDR4 knockdown inhibited proliferation and migration in lung cancer cells**

(A and B) Western blot confirmation of WDR4 knockdown using two independent shRNAs in A549 and H1299 cells. (C and D) Cell proliferation of A549 and H1299 cells was suppressed by WDR4 knockdown. (E and F) Knockdown of WDR4 inhibited colony formation in A549 and H1299 cells. (G and H) Wound-healing assay revealed the inhibitory activity of WDR4 knockdown on cell migration. (I and J) Knockdown of WDR4 inhibited A549 and H1299 cell invasion. Data were presented as mean  $\pm$  SD. Scale bar, 100  $\mu$ m. (One-way ANOVA, \* $p$  < 0.05, \*\* $p$  < 0.01, \*\*\* $p$  < 0.001, compared to the shGFP group.)

### Knockdown of METTL1/WDR4 inhibits tumor growth *in vivo*

We next performed xenograft tumor-formation assays to evaluate the functions of METTL1/WDR4 in regulation of lung cancers *in vivo*. Briefly, METTL1 knockdown and control A549 cells were subcutaneously injected into the right dorsal flank of nude mice, and the tumor volumes were measured weekly. Our results showed that larger subcutaneous visible tumors were observed in the control group, whereas only 3 smaller subcutaneous tumors were found in the shM1-1 group, and no subcutaneous tumor was found in the shM1-2 group (Figure 4A). Xenograft tumor growth curve and tu-

mor weight also revealed that METTL1 knockdown significantly reduces tumor growth *in vivo* (Figures 4B and 4C). IHC analysis confirmed the reduced expression of METTL1 and WDR4 in xenograft tumors from shMETTL1 (shM1) groups (Figures 4D and 4E). In addition, xenograft tumors from shM1 groups showed lower Ki67 expression level, suggesting that METTL1-knockdown xenograft tumors were less malignant than those of the control group (Figure 4F). To further study the role of tRNA m<sup>7</sup>G modification on lung cancer progression, we also performed the xenograft tumor-formation assays with WDR4-knockdown A549 cells.

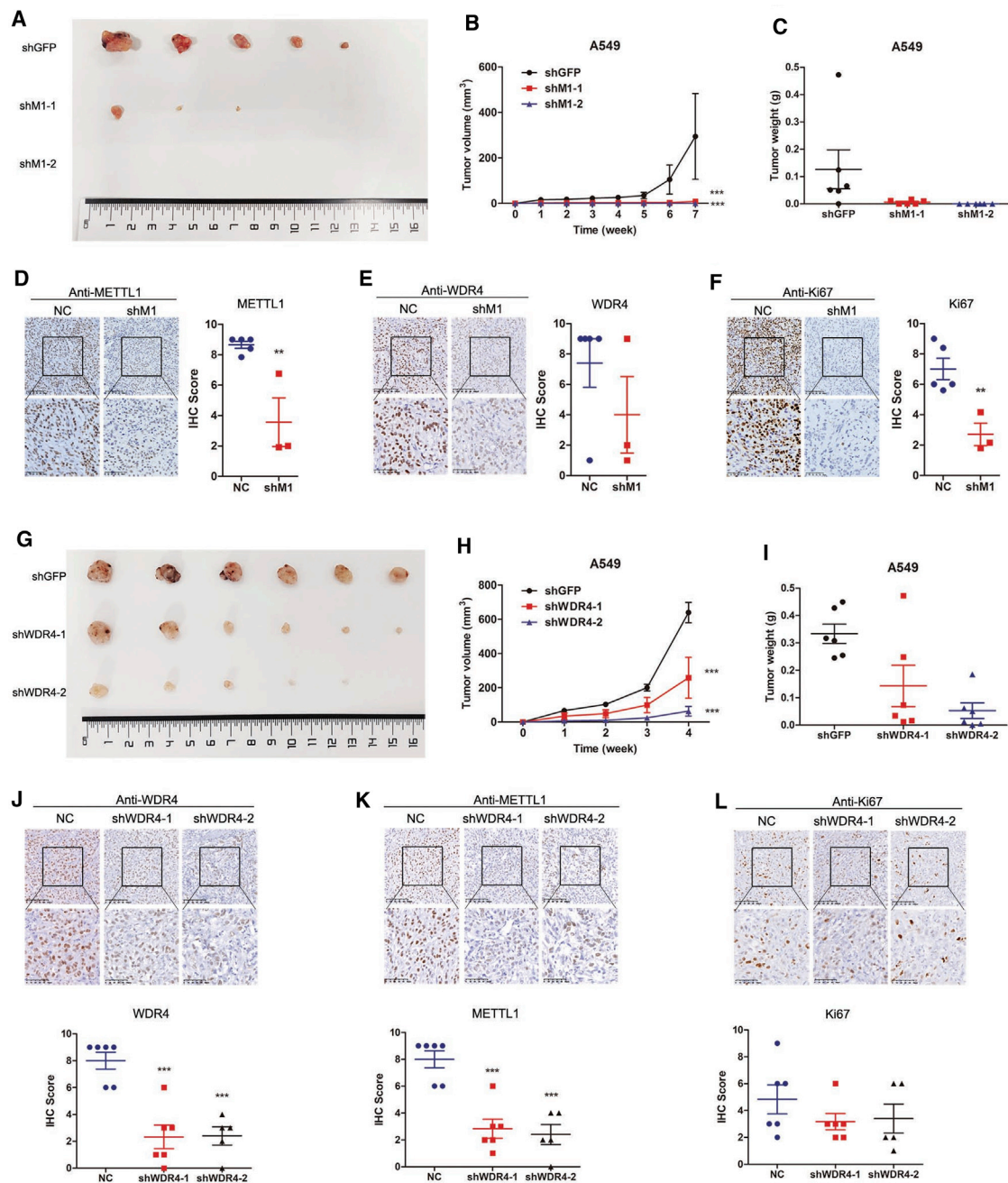


**Figure 4. Knockdown of METTL1/WDR4 inhibited tumor growth *in vivo***

(A) METTL1-depleted A549 cells formed less and smaller xenograft tumors *in vivo* experiments (n = 6). (B and C) Growth curve (B) and final tumor weights (C) of xenograft tumors induced by A549 cells with or without METTL1 depletion. (D–F) Representative IHC staining images and quantitative IHC staining scores of METTL1 (D), WDR4 (E), and Ki67 (F) in xenograft tumors. (G) WDR4-depleted A549 cells formed less and smaller xenograft tumors in *in vivo* experiments (n = 6). (H and I) Growth curve (H) and final tumor weights (I) of xenograft tumors induced by A549 cells with or without WDR4 depletion. (J–L) Representative IHC staining images and quantitative IHC staining scores of WDR4 (J), METTL1 (K), and Ki67 (L) in xenograft tumors. Data were presented as mean ± SEM. Scale bars, 100 μm and 50 μm. (Two-way ANOVA, one-way ANOVA, Student's t test, \*\*p < 0.01, \*\*\*p < 0.001, compared to the shGFP group.)

Similarly, knockdown of WDR4 significantly suppressed lung cancer progression in the xenograft tumor model, as reflected by the reduced tumor size and tumor weight (Figures 4G–4I). Expression

of METTL1 and WDR4 was reduced in xenograft tumors from shWDR4 groups (Figures 4J and 4K). In addition, WDR4-depleted tumors were less proliferative as revealed by reduced expression of

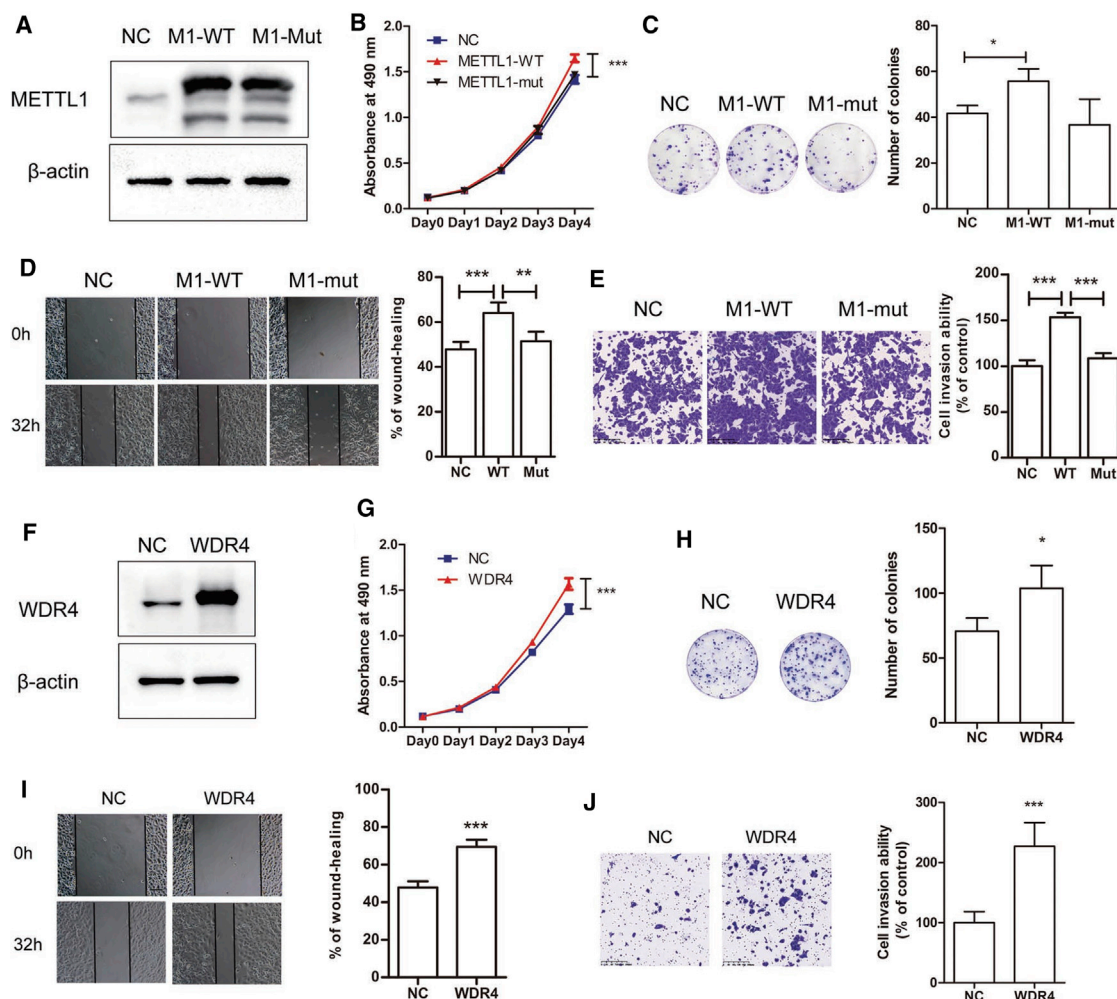


**Figure 5. Overexpressed METTL1/WDR4 promoted cell growth and invasion in A549 cells**

(A) Western blot confirmation of METTL1 upregulation in A549 cells. (B) Overexpressed METTL1 promoted cell growth in A549 cells. (C) Overexpression of wild-type METTL1 instead of catalytic mutant METTL1 promoted cell colony formation in A549. (D and E) Overexpressed METTL1 promoted migration (D) and invasion (E) of A549 cells. (F) Western blot confirmation of WDR4 upregulation in A549 cells. (G) Overexpressed WDR4 promoted cell growth in A549 cells. (H) Overexpression of WDR4 promoted cell colony formation in A549. (I and J) Overexpressed WDR4 promoted migration (I) and invasion (J) of A549 cells. Data were presented as mean  $\pm$  SD. Scale bars, 100  $\mu$ m (D and I); 200  $\mu$ m (E and J). (Two-way ANOVA, Student's *t* test, \*\**p* < 0.01, \*\*\**p* < 0.001, compared to the negative control [NC] group.)

Ki67 (Figure 4L). Taken together, our *in vitro* and *in vivo* assays supported that METTL1 and WDR4 were crucial in the regulation of lung cancer progression.

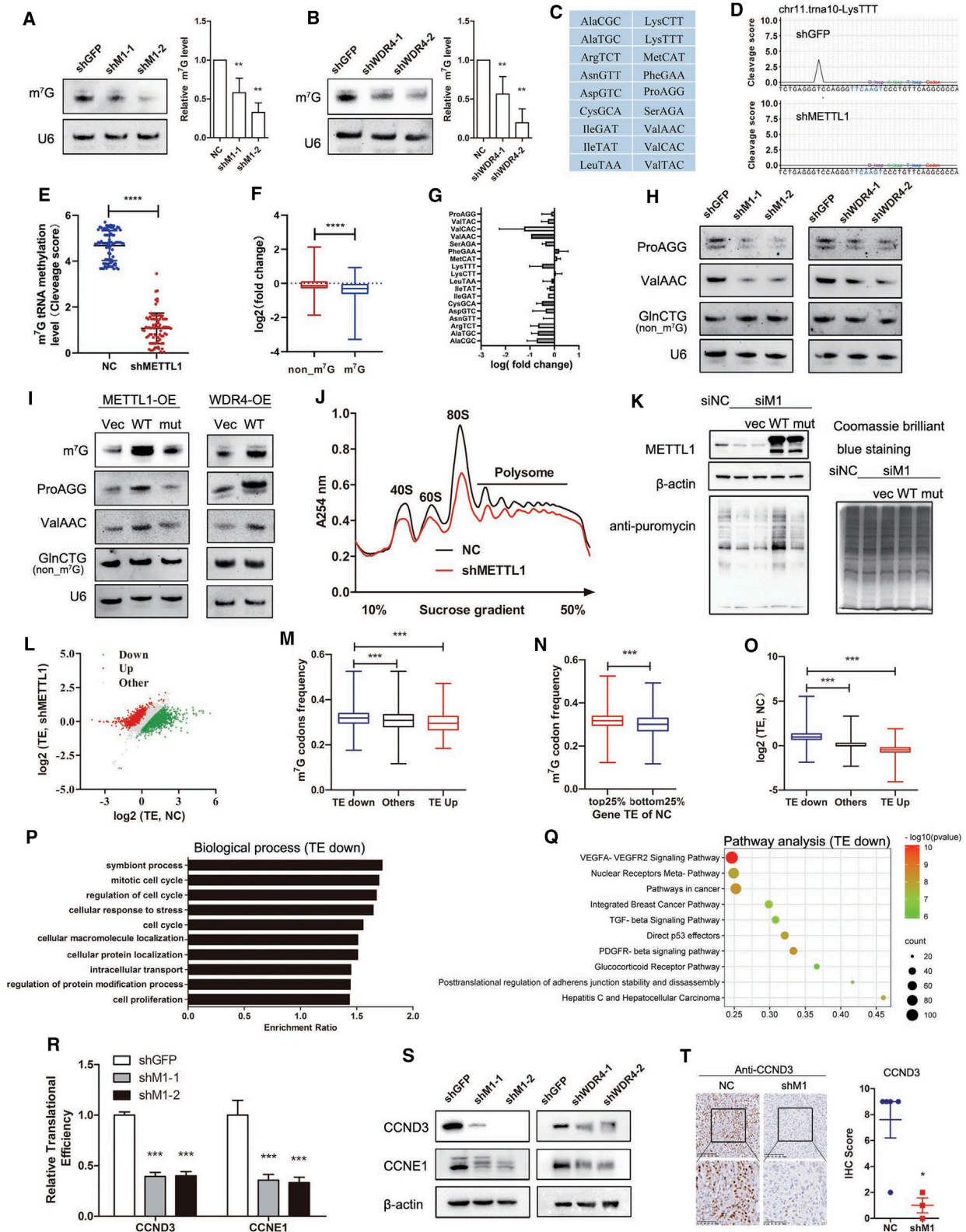
#### Overexpression of METTL1/WDR4 promotes lung cancer cell growth and invasion capacities

In order to further validate the function METTL1/WDR4-mediated  $m^7G$  tRNA modification in lung cancer progression, we next performed gain-of-function studies in lung cancer cells. Results showed that overexpression of wild-type METTL1 (M1-WT) significantly promotes the cell proliferation and colony formation of lung cancer cells (Figures 5A–5C). In addition, migration and invasion capacities of lung cancer cells were also enhanced by METTL1 overexpression (Figures 5D and 5E). However, overexpression of the catalytic dead

mutant METTL1 (M1-Mut) had little function on lung cancer progression (Figures 5A–5E), suggesting that METTL1's enzyme activity is essential for its function in promoting lung cancer progression. Moreover, overexpression of WDR4 also promoted cell growth, colony formation, migration, and invasion in lung cancer cells (Figures 5F–5J). Taken together, these results demonstrate that METTL1/WDR4 and their mediated  $m^7G$  tRNA modification are critical for lung cancer progression.

#### METTL1 depletion reduces tRNA $m^7G$ modification and expression

In order to unveil the mechanisms underlying how METTL1 regulates lung cancer progression, we first performed a northwestern blot to analyze the  $m^7G$  modification level and found a notable



(legend on next page)



reduction in tRNA m<sup>7</sup>G modification in METTL1-depleted or WDR4-depleted cells in lung cancer cells (Figures 6A and 6B; Figure S1B). We next performed tRNA reduction and cleavage sequencing (TRAC-seq) to profile m<sup>7</sup>G modification in tRNAs in lung cancer cells after METTL1 knockdown. Briefly, total RNAs were extracted, and small RNAs were isolated and subjected to DNA oxidative demethylase AlkB demethylation and then reduced and cleaved by NaBH<sub>4</sub>/aniline treatment. Following purification, the purified RNAs were used for high-throughput sequencing to identify global tRNA m<sup>7</sup>G modifications at single-nucleotide resolution. Our TRAC-seq result identified a series of tRNA isoacceptors containing m<sup>7</sup>G modification in A549 lung cancer cells (Figure 6C). METTL1 depletion decreased m<sup>7</sup>G modification levels in tRNAs as reflected by reduced cleavage scores (Figures 6D and 6E). Analysis of tRNA expression revealed that METTL1 knockdown decreased the expression of the majority of m<sup>7</sup>G-modified tRNAs (Figures 6F and 6G). Northern blot analysis confirmed that the METTL1 and WDR4 knockdown reduced the expression of m<sup>7</sup>G-modified tRNAs ValAAC and ProAGG but not the non-m<sup>7</sup>G-modified tRNA GlnCTG (Figure 6H). On the other hand, overexpression of wild-type METTL1 and WDR4 upregulated tRNA m<sup>7</sup>G modification and enhanced the expression of m<sup>7</sup>G-modified tRNAs ValAAC and ProAGG but not the non-m<sup>7</sup>G tRNA GlnCTG (Figure 6I). Overall, these results revealed that METTL1 and WDR4 are essential for tRNA m<sup>7</sup>G modification and expression.

### METTL1 depletion inhibits mRNA translation

Given that tRNAs are essential factors for mRNA translation, we further determined whether m<sup>7</sup>G tRNA modification was involved in the regulation of mRNA translation in lung cancer cells. Polysome profiling revealed that METTL1 knockdown results in reduction of polysome fractions (Figure 6J), suggesting the decreased mRNA translation activities in the METTL1-depleted cells. In addition, puromycin-intake assay, a method to monitor new protein synthesis rate, also confirmed that METTL1 depletion reduces global mRNA translation efficiency (TE) in lung cancer cells (Figure 6K). Overexpression of wild-type instead of catalytic inactive mutant METTL1 rescued the puromycin-intake ef-

iciency of lung cancer cells, indicating the crucial role of METTL1's catalytic activity in regulation of mRNA translation (Figure 6K).

We further applied ribosome nascent-chain complex (RNC)-bound mRNA sequencing (RNC-mRNA-seq) to profile mRNA translation in METTL1-depleted and control cells. Our RNC-mRNA-seq identified 2,331 genes with decreased TE (TE down) and 1,179 genes with increased TE (TE up) in METTL1-depleted lung cancer cells (Figure 6L; Tables S2–S4). Further analysis found significant correlation between m<sup>7</sup>G codon frequency and altered TE of mRNAs: the TE of mRNAs with higher frequency of m<sup>7</sup>G codon decreased upon METTL1 knockdown; on the other hand, mRNAs with lower m<sup>7</sup>G codon frequency have upregulated TE, suggesting that METTL1-mediated tRNA m<sup>7</sup>G modification regulates mRNA translation in a m<sup>7</sup>G codon-dependent mechanism (Figure 6M). Moreover, analysis of the correlation between mRNA TE and m<sup>7</sup>G codon composition revealed that highly translated mRNAs (top 25% in TE) have significantly higher frequencies of m<sup>7</sup>G tRNA codons than the mRNAs with low TEs (bottom 25% in TE) in A549 lung cancer cells, suggesting that m<sup>7</sup>G tRNA codons could be the optimal codons used in the highly translated mRNAs (Figure 6N). We further analyzed the TEs of the mRNAs induced or downregulated in response to shM1 and found that METTL1 knockdown decreases the TE of highly translated mRNAs (Figure 6O), further supporting important function of METTL1-mediated m<sup>7</sup>G tRNA modification and the usage of m<sup>7</sup>G codons in promoting mRNA translation. Gene ontology and pathway analysis revealed that mRNAs with TE down are enriched in cell-cycle regulation and cancer pathways (Figures 6P and 6Q). RNC-quantitative reverse transcriptase PCR (qRT-PCR) assays confirmed that the TE of cell-cycle regulators CCND3 and CCNE1 were significantly decreased in shM1 cells (Figure 6R). Consistently, western blot revealed that knockdown of METTL1 decreased the protein levels of CCND3 and CCNE1 (Figure 6S). We further detected the expression levels of CCND3 in xenograft tumors and revealed that CCND3 expression levels were decreased in METTL1- or WDR4-depleted xenograft tumors (Figure 6T; Figure S2). Taken together, our data uncovered that METTL1/WDR4-mediated tRNA m<sup>7</sup>G modification regulates mRNA translation in lung cancer cells.

### Figure 6. METTL1 depletion reduced tRNA m<sup>7</sup>G modification, m<sup>7</sup>G tRNA expression, and oncogenic mRNA translation

(A and B) m<sup>7</sup>G modification decreased in A549 lung cancer cells with METTL1 or WDR4 depletion. (C) The list of m<sup>7</sup>G-modified tRNAs in A549 cells identified by TRAC-seq. (D) Representative images of cleavage scores of indicated tRNAs at m<sup>7</sup>G-modified sites. Decreased cleavage score was shown in the shMETTL1 group, indicating the reduced m<sup>7</sup>G modification level in METTL1-depleted cells. (E) tRNA m<sup>7</sup>G modification level was decreased in METTL1-depleted A549 cells. (F) m<sup>7</sup>G-modified tRNAs expression levels were decreased in METTL1-depleted A549 cells compared to that of the non-m<sup>7</sup>G-modified tRNAs. (G) Relative expression profile of m<sup>7</sup>G-modified tRNAs based on TRAC-seq. The relative expression of each tRNA type was calculated from the combined expression of all of the tRNA genes belonging to the same tRNA type. (H) Northern blotting analyzed the expression levels of representative m<sup>7</sup>G-modified tRNAs and non-m<sup>7</sup>G-modified tRNAs in lung cancer cells upon METTL1 or WDR4 depletion. U6 snRNA was used as a loading control. (I) Overexpression of METTL1 or WDR4 increased the expression level of m<sup>7</sup>G modification and m<sup>7</sup>G-modified tRNAs in lung cancer cells. (J) Polysome profiling of A549 cells with or without METTL1 knockdown. (K) Translation efficiency (TE) of METTL1-depleted A549 cells was decreased by analyzing the puromycin intake in cells. Overexpression of wild-type METTL1 instead of catalytic inactive mutant METTL1 rescued translation deficiency of METTL1-depleted A549 cells. (L) Scatterplot of gene TE in A549 cells with or without METTL1 depletion. TE was calculated by dividing the RNC-mRNA sequencing signals to input mRNA sequencing signals. (M) Frequency of the m<sup>7</sup>G-related codons in TE up, TE down, and other genes (others) in METTL1 depletion cells. (N) m<sup>7</sup>G codon frequency of genes with the top 25% TE was significantly higher than that of the genes with the bottom 25% TE in the NC group. (O) TEs of the identified TE down gene were significantly higher than that of the other and TE up genes in NC cells. (P) Gene ontology analysis of function enrichment in the biological process with TE down genes in METTL1 depletion cells. (Q) Pathway analysis with TE down genes in METTL1 depletion cells. (R and S) qRT-PCR and western blotting confirmed the TEs changes of the identified cell-cycle-related genes. (T) IHC confirmed the decreased expression of the identified TE down gene CCND3 in METTL1-depleted xenograft tumors sections. Data were presented as mean ± SD. Scale bars, 100 μm and 50 μm. (One-way ANOVA, Student's t test, \*p < 0.05, \*\*\*p < 0.001, compared to the shGFP group.)

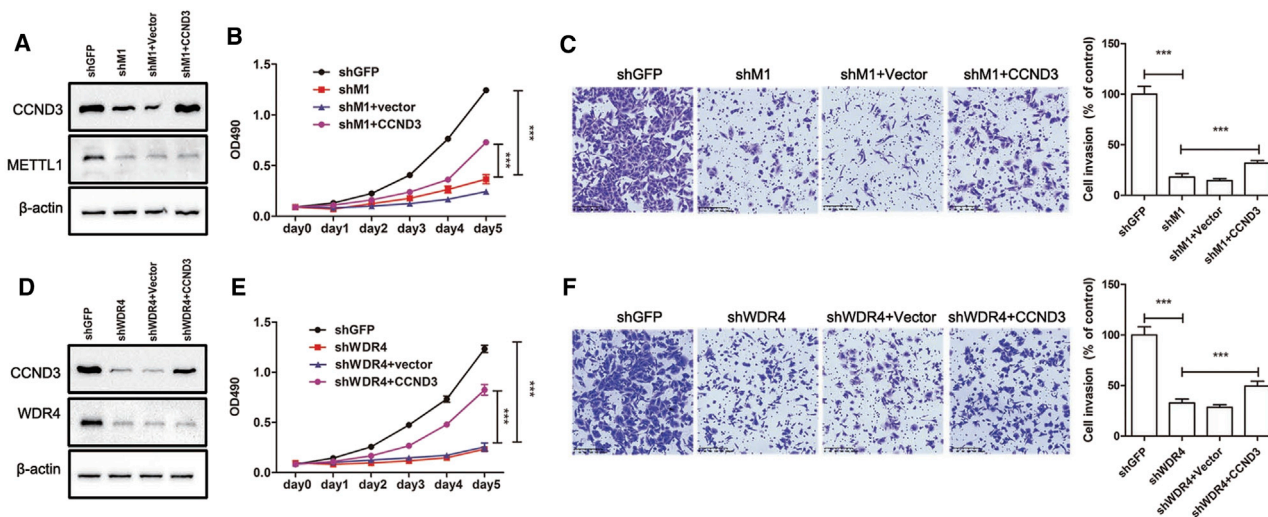


**Figure 7. CCND3 overexpression partially rescues cancer cell phenotypes in METTL1/WDR4-depleted A549 cells**

(A) Validation of the CCND3 overexpression in METTL1-depleted A549 cells. (B and C) Overexpression of CCND3 partially rescued the growth (B) and invasion capacity (C) of METTL1-depleted A549 cells. (D) Validation of the CCND3 overexpression in WDR4-depleted A549 cells. (E and F) Overexpression of CCND3 partially rescued the growth (E) and invasion capacity (F) of WDR4-depleted A549 cells. Data were presented as mean  $\pm$  SD. Scale bar, 200  $\mu$ m. (One-way ANOVA, two-way ANOVA, \* $p < 0.05$ , \*\*\* $p < 0.001$ .)

### CCND3 overexpression partially rescues cancer cell phenotypes in METTL1/WDR4-depleted A549 cells

Results mentioned above showed that METTL1 knockdown results in translation defects of mRNAs enriched in cell-cycle and cancer pathways. To further confirm these results, we overexpressed the METTL1 downstream target CCND3 in METTL1-depleted lung cancer cells (Figure 7A). Our results revealed that overexpression of CCND3 could partially rescue the cell growth and invasion capacities of METTL1-depleted A549 cells (Figures 7B and 7C). Similarly, CCND3 overexpression can also partially rescue the growth and invasion of WDR4-depleted cells (Figures 7D–7F). Overall, our data provide strong evidence supporting the essential function of METTL1/WDR4-mediated tRNA  $m^7G$  modification in regulation of mRNA translation and lung cancer progression.

### DISCUSSION

The tRNAs are the most heavily modified RNA species that recognize mRNA codons and bridge corresponding amino acids during protein synthesis.<sup>4–6</sup> The accurate tRNA modifications are crucial for efficient protein translation.<sup>7,8</sup> Recent research advances uncovered the critical role of tRNA modifications and translation regulation in disease development and cancer progression.<sup>9,10,24–26</sup> The  $m^7G$  modification occurs in the variable loops of tRNAs and is highly conserved between different species.<sup>15–17</sup> Although  $m^7G$  modifications in tRNAs are nonessential for yeast growth under normal condition,<sup>23</sup> mutations of the human tRNA  $m^7G$  methyltransferase complex often result in developmental defects such as brain disorders.<sup>18–21</sup> Consistently, our recent study revealed that METTL1 or WDR4 knockout results in defected self-renewal capacity and a disordered differentiation program of mouse embryonic stem cells,<sup>16</sup> suggesting the important phys-

iological functions of tRNA  $m^7G$  modifications in the mammalian systems.

Although tRNA  $m^7G$  modification has been reported to play important functions in embryonic stem cells, its role in cancers remains poorly understood. Recent studies found that tRNA  $m^7G$  methyltransferase METTL1 is overexpressed in cancers and correlated with poor patient prognosis and chemoresistance, suggesting the potential functions of METTL1 in cancer biology,<sup>17,27,28</sup> whereas the molecular insights are still poorly understood. In the present study, we aimed to demonstrate the function of METTL1-mediated tRNA  $m^7G$  modifications in lung cancer. We found that both subunits of the tRNA  $m^7G$  modification catalytic complex, METTL1 and WDR4, are upregulated in lung cancers. Depleting either METTL1 or WDR4 suppressed lung cancer cell proliferation, colony formation, cell invasion, and *in vivo* tumor progression. Further study revealed that METTL1 and WDR4 played an oncogenic role in lung cancer via mediating  $m^7G$  tRNA modification and modulated the translation of mRNAs including cell-cycle genes. Our data supported that METTL1/WDR4-mediated  $m^7G$  tRNA modification served as an oncogenic factor in lung cancer.

Our RNC-mRNA-seq revealed that the TEs of mRNAs with higher frequency of modified  $m^7G$  codons are inhibited in METTL1-depleted lung cancer cells. Analysis of the basal TEs in lung cancer cells revealed that the highly translated mRNAs contain significantly higher frequencies of  $m^7G$  codons than the mRNAs with low TEs, suggesting that the  $m^7G$  codons are more optimal for efficient mRNA translation in lung cancers.<sup>29,30</sup> In addition, the TEs of the highly translated mRNAs are downregulated by METTL1 depletion,

suggesting that METTL1-mediated m<sup>7</sup>G tRNA modification and m<sup>7</sup>G codon usage promote mRNA translation and lung cancer progression. This uncovered new insights into mRNA translation enhancement through tRNA modifications and the corresponding codon compositions in lung cancers.

In summary, the present study demonstrates the essential function and molecular mechanisms underlying METTL1/WDR4 and their mediated m<sup>7</sup>G tRNA modifications in regulation of mRNA translation and lung cancer progression. Our data uncovered tRNA m<sup>7</sup>G modifications as important oncogenic factors and provided profound molecular insights into oncogene translation in cancers.

## MATERIALS AND METHODS

### RNA expression and survival analysis using TCGA databases

The RNA expression data for lung cancer were downloaded from TCGA databases (<https://portal.gdc.cancer.gov/>) and log<sub>2</sub> transformed to analyze the expression of METTL1 and WDR4 in lung cancer and normal lung tissues. The prognostic role of METTL1 and WDR4 was analyzed by querying the Kaplan-Meier Plotter database (<http://kmplot.com/analysis/>).

### Patient samples

Commercial lung cancer tissue array (HLugA150CS02 specs; US Biomax, USA) containing 75 cases lung cancer tissues and their paired peri-tumor normal tissues was subjected to IHC analysis of the METTL1 expression. Frozen tissues were obtained from lung cancer patients who had curative resections at The First Affiliated Hospital of Sun Yat-Sen University and were used for analysis of the protein levels of METTL1 and WDR4 and m<sup>7</sup>G tRNA modification level. Written consent was obtained from each patient. Ethical approval for research on human subjects was obtained from the Institutional Review Board of The First Affiliated Hospital of Sun Yat-Sen University.

### Cell culture

Lung cancer cell lines A549 and NCI-H1299 were cultured in DMEM supplemented with 10% fetal bovine serum (FBS) and 1% penicillin-streptomycin and incubated in a humidified incubator with 5% carbon dioxide (CO<sub>2</sub>) at 37°C. After infected with lentiviruses containing shGFP (NC group), shM1, or shWDR4, cells were subjected to different assays to investigate the biological functions of METTL1 or WDR4 in lung cancer cells. The shRNA sequences used in this study were listed in [Table S1](#). For gain-of-function assays and rescues assays, gene expression plasmids were transfected into cells with Lipofectamine 2000 Transfection Reagent (Thermo Fisher Scientific, USA), and then cells were subjected to different assays.

### Plasmid construction

Gene expression plasmids were generated by cloning the open reading frames of the human WDR4 gene (GenBank: NM\_005228.5) and CCND3 gene (GenBank: NM\_001136017.3) into the pFLAG-CMV2 plasmid. The wild type and catalytic inactive mutant

(amino acids [aa] 160–163, LFPD to AFPA) METTL1 expression plasmids were previously generated.<sup>16</sup>

### MTT assay and cell-cycle analysis

Cells were seeded in 96-well plates at a density of 1,000 cells/well and cultured for 5 days. MTT assay was applied to evaluate cell proliferation at indicated time points. Briefly, MTT was dissolved in PBS to 5 mg/mL stock solution and then sterilized with a 0.22- $\mu$ m filter. At indicated time points, cell culture medium was carefully removed, and then 90  $\mu$ L cell culture medium mixed with 10  $\mu$ L MTT stock solution was added into each well, which then incubated for 3 h at 37°C. After that, we removed the medium, added 100  $\mu$ L dimethyl sulfoxide (DMSO) to each well, and shook the cell-culture plate in the dark for 10 min. Cell proliferation was determined by reading the plates at optical density 490 (OD<sub>490</sub>) nm. For cell-cycle analysis, cells seeded in 6-well plates (70%–80% confluence) were harvested after treatment with trypsin without EDTA. Following two washes with PBS, cells were resuspended and fixed in cold 70% ethanol overnight at 4°C. Cell-cycle analysis was performed according to the manufacturer's instruction of the Cell Cycle Assay Kit (Dojindo, China) with a CytoFLEX flow cytometer (Beckman Coulter, USA).

### Cell colony formation

Cells (250 cells/well) were seeded in a 6-well plate and cultured for 2 weeks. After being washed twice with PBS, cells were fixed with 4% formaldehyde and stained with 0.1% crystal violet solution. Cell colonies (>50 cells per colony) were counted to evaluate the colony-formation capacities of lung cancer cells.

### Cell migration and invasion assay

To test the effect of METTL1 on lung cancer cell metastasis, cell invasion assays were performed using a BD BioCoat Matrigel Invasion Chamber (8  $\mu$ m pore size) (BD Biosciences, USA).  $1 \times 10^5$  cells were suspended in serum-free medium and added to the upper face of the cell culture chambers. The chambers were placed into a 24-well plate containing DMEM supplemented with 10% FBS. After incubation for indicated times (20 h for A549 and 24 h for NCI-H1299 cells, respectively), cells in the upper face of the chambers were scraped, and cells adhering on the lower surface of the chambers were fixed, stained with crystal violet, and photographed with a microscope (ZEISS Axio Observer Z1; Zeiss, Jena, Germany).

A wound-healing assay was performed to analyze cell migration *in vitro*. Cells ( $6 \times 10^5$  per well) were seeded in a 12-well plate and allowed to adhere to the plate completely. Scratch wounds were created in the nearly 100% confluent cells in each well with a pipette tip. Then cells were cultured in DMEM supplemented with 2% FBS. Scratch wounds were captured with a microscope at indicated time points.

### Polysome profiling

For polysome profiling analysis, cell culture medium was removed from cells (70%–80% confluence,  $3 \times 150$  mm cell culture plates);

then cells in the culture plates were quickly washed with ice-cold PBS containing 100 µg/mL cycloheximide. Cells were then collected and lysed in 1.2 mL polysome extraction buffer (50 mM 3-(N-morpholino)propanesulfonic Acid [MOPS], 15 mM MgCl<sub>2</sub>, 150 mM NaCl, 100 µg/mL cycloheximide, 0.5% Triton X-100, 1 mg/mL heparin, 40 U/mL RNaseOUT, 2 mM PMSF, and 1 mM benzamidine) on ice for 10 min. Cell lysates were centrifuged at 13,000 × *g* for 10 min. 1 mL clarified supernatant of each samples was transferred onto the top of 10%–50% sucrose gradient solution (50 mM MOPS, 15 mM MgCl<sub>2</sub>, 150 mM NaCl, and 100 µg/mL cycloheximide) and centrifuged at 36,000 rpm for 2.5 h at 4°C for gradient sedimentation analysis. Gradient fractions were collected from the top of 10%–50% sucrose gradient solution using gradient fractionators, with measurement of absorbance at 254 nm.

### RNC-mRNA-seq and data analysis

To examine the alteration of mRNA translation after METTL1 depletion, we performed mRNA-seq on total mRNAs and RNC-mRNAs from METTL1-depleted or controlled A549 cells. RNC-mRNAs were extracted as described previously.<sup>31</sup> Cells were quickly washed with ice-cold PBS containing 100 µg/mL cycloheximide and then collected and lysed in 1.2 mL lysis buffer containing 1% Triton X-100 in ribosome buffer (RB buffer; which contains 20 mM HEPES-KOH [pH 7.4], 15 mM MgCl<sub>2</sub>, 200 mM KCl, 100 µg/mL cycloheximide, and 2 mM dithiothreitol) for 30 min on ice. Cell lysates were subjected to centrifuge at 16,200 × *g* for 10 min at 4°C to remove the cell debris. The supernatants were transferred on the surface of 12 mL of RB buffer containing 30% sucrose. RNC-mRNAs were pelleted after ultra-centrifugation at 185,000 × *g* for 5 h at 4°C. RNAs in total cell lysates and RNC-mRNAs were extracted with Trizol reagent and subjected to RNA sequencing (RNA-seq).

The gene-expression level was normalized using TPM (transcripts per kilobase of exon model per million mapped reads). The TEs were calculated using the following formula: TE = (TPM in RNC sequencing [RNC-seq])/(TPM in input RNA-seq). Genes with a TE ratio of shM1/NC less than 0.667 and more than 1.5 were classified as TE down and TE up, respectively. The identified TE down genes were subjected to gene ontology analysis using WEB-based Gene Set Analysis Toolkit (<http://www.webgestalt.org/>) and pathway analysis using the ToppGene Suite (<https://toppgene.cchmc.org/enrichment.jsp>).

### Real-time qRT-PCR

Total RNA samples were extracted using Trizol reagent following the manufacturer's instructions. For reverse transcription, 1 µg RNA of each sample was used to synthesize the first-strand cDNA using the PrimeScript RT Master Mix (Takara, Japan). qRT-PCR assays were then performed with LC480 (Roche, USA) utilizing SYBR Premix Ex Taq II (Takara, Japan). β-actin was chosen as an endogenous control to normalize the target gene expression levels in different groups. The relative mRNA expression levels of target genes were calculated using the 2<sup>-ΔΔCt</sup> method. The primer sequences used in this study were listed in Table S1.

### TRAC-seq and data analysis

To profile m<sup>7</sup>G tRNA modifications in lung cancer cells after METTL1 knockdown, TRAC-seq was performed as described.<sup>32</sup> Total RNA samples were first extracted from A549 cells with or without METTL1 depletion using the Trizol reagent and then subjected to small RNA purification using the mirVana miRNA Isolation Kit. The isolated small RNAs were demethylated with recombinant ALKB-wild-type and ALKB-D135S demethylases treatment. The demethylated small RNAs were then treated with 0.2 M NaBH<sub>4</sub> on ice for 30 min in the dark and purified using the Oligo Clean & Concentrator Kit (Zymo Research, USA). The NaBH<sub>4</sub>-treated small RNAs were subsequently incubated with 100 µL cleavage buffer (H<sub>2</sub>O:glacial acid:aniline = 7:3:1) at room temperature in the dark for 2 h. After purification with the Oligo Clean & Concentrator Kit, the small RNAs were subjected to cDNA library construction using the NEBNext Multiplex Small RNA Library Prep Set for Illumina Kit (New England Biolabs, USA), followed by high-throughput sequencing.

The m<sup>7</sup>G-modified sites were identified using methods as previously described.<sup>16,32</sup> First, the referenced human tRNA sequences were downloaded from the GtRNAdb database (<http://gtRNadb.ucsc.edu/genomes/eukaryota/Hsapi38/>). For analysis of tRNA modification and expression, the introns in the tRNA gene sequences were removed to obtain the mature tRNA sequence, and then the “CCA” sequence was added to the 3' end of all mature tRNA sequences. For analysis of m<sup>7</sup>G tRNA modifications, clean reads from the NaBH<sub>4</sub>/aniline chemical-treated sequencing reads and the control input sequencing reads were trimmed to remove the adaptor sequence used during library construction. Then the trimmed reads were mapped to the CCA-added mature tRNA sequences using Bowtie (<http://bowtie-bio.sourceforge.net>). After that, Bedtools (<https://bedtools.readthedocs.io/en/latest>) was applied for analyzing the ratio of the number of reads starting at the chemical treatment-induced cleaved sites to the read depth of the site. For specific m<sup>7</sup>G-modified site *i*, the cleavage ratio of site *i* was calculated as the ratio between the number of reads starting at site *i* and the read depth of site *i*. Then, the cleavage score of site *i* was calculated as previously described:<sup>32</sup>

$$\text{Cleavage score}_i = \frac{\log_2(\text{Cleavage ratio}_{\text{treat}})}{\log_2(\text{Cleavage ratio}_{\text{non\_treat}})}$$

For analysis of tRNA expression, AlkB-treated tRNA sequencing data were used. The clean data were mapped to the CCA-added human mature tRNA sequences using Bowtie2. Then the read counts of tRNA were calculated and normalized using the programs based on the AlkB-facilitated RNA methylation sequencing (ARM-seq) data analysis pipeline.<sup>32,33</sup>

### Northwestern blot

To detect the variation of m<sup>7</sup>G modifications in tRNAs, a northwestern blot was performed as previously described.<sup>16</sup> After being heat denatured at 95°C for 5 min, 2 µg total RNAs were loaded on 15% polyacrylamide Tris-borate-EDTA (TBE) urea gel for

electrophoresis in  $1 \times$  TBE buffer to separate RNAs by molecular weight. RNAs were then transferred onto a positive-charged nylon membrane and crosslinked with a UVP crosslinker (Analytik Jena, USA). And  $m^7G$  modification signal of RNAs was detected following the western blot protocol with anti- $m^7G$  antibody (MBL International; #RN017M).

#### Western blot

Cells were lysed with RIPA buffer containing 1 mM PMSF and proteinase inhibitor cocktail. After separation with 12.5% SDS-PAGE, proteins were transferred onto a polyvinylidene fluoride (PVDF) membrane. The membranes were then blocked with 5% milk in TBST and incubated with indicated primary antibodies overnight at 4°C. Following three washes in TBST, the membranes were incubated with respective secondary horseradish peroxidase (HRP)-conjugated antibody at room temperature for 1 h and washed with TBST. The immunoreaction signals were detected with enhanced chemiluminescence HRP substrate (Millipore, USA).

#### Puromycin intake assay

Cells were transfected with METTL1 small interfering RNA (siRNA) and NC (siNC) oligos. 48 h after transfection, cells were incubated with puromycin (1  $\mu$ M final concentration) for 30 min and then lysed in RIPA buffer. Protein lysis was subjected to western blot to analyze the puromycin intake. The siRNA sequences used in this study were listed in [Table S1](#).

#### IHC assay

The protein level of METTL1 in lung cancer tissues was investigated using a tissue array by IHC with an antibody against METTL1 (Proteintech; 14994-1-AP, 1:2,000 dilution) and evaluated by a semiquantitative IRS. The staining intensity was scored as 0 (absent), 1 (weak), 2 (moderate), and 3 (strong), and the proportion of positive staining cells was scored as 0, 1, 2, and 3 for absent, <10%, 10% to 50%, and >50%, respectively. The product of intensity score and proportion score resulted in an IRS index and was used to evaluate the immunoreactivity of METTL1. Lung cancer tissues with  $IRS \geq 3$  were divided into the high METTL1 expression group, and tissues with  $IRS < 3$  were divided into the low METTL1 expression group.

#### In vivo tumorigenic assays

To evaluate the tumorigenic ability of A549 cells after knockdown of METTL1 or WDR4, a xenograft experiment was performed with the approval of the Ethics Committees of The First Affiliated Hospital of Sun Yat-Sen University.  $1 \times 10^6$  cells were subcutaneously injected into the right dorsal flank of nude mice (six mice per group), and the tumor volume was measured weekly. The tumor volume was presented as a product of  $0.5 \times \text{length} \times \text{width}^2$ . At the end of the experiment, animals were sacrificed, the tumors were harvested, and the weight of tumors was measured.

#### Data analysis and availability

Statistical analysis was performed in GraphPad Prism 5 software with details added to figure legends. The accession number of raw

sequencing data deposited to the NCBI Gene Expression Omnibus (GEO) is GEO: GSE173761.

#### SUPPLEMENTAL INFORMATION

Supplemental information can be found online at <https://doi.org/10.1016/j.ymthe.2021.08.005>.

#### ACKNOWLEDGMENTS

This work was supported by the National Natural Science Foundation of China (81922052, 81974435, 81772999, and 82002981), Distinguished Young Scholars Grant from Natural Science Foundation of Guangdong (2019B151502011), Guangzhou People's Livelihood Science and Technology Project (201903010006), and Medical Scientific Research Foundation of Guangdong Province (A2018022).

#### AUTHOR CONTRIBUTIONS

T.C., L.H., Y.L., W.L., and S.L. conceived the study, designed the experiments, and supervised the project. J.M., H.H., Y.H., C.Y., S.Z., J.B., X.H., and R.L. performed experiments and acquired and analyzed the data. Y.L., W.L., and S.L. wrote the manuscript with input from all authors.

#### DECLARATION OF INTERESTS

The authors declare no competing interests.

#### REFERENCES

1. Siegel, R.L., Miller, K.D., and Jemal, A. (2018). Cancer statistics, 2018. *CA Cancer J. Clin.* 68, 7–30.
2. Chao, Y.L., and Pecot, C.V. (2021). Targeting Epigenetics in Lung Cancer. *Cold Spring Harb. Perspect. Med.* 11, a038000.
3. Tahmasebi, S., Khoutorsky, A., Mathews, M.B., and Sonenberg, N. (2018). Translation deregulation in human disease. *Nat. Rev. Mol. Cell Biol.* 19, 791–807.
4. Machnicka, M.A., Olchowik, A., Grosjean, H., and Bujnicki, J.M. (2014). Distribution and frequencies of post-transcriptional modifications in tRNAs. *RNA Biol.* 11, 1619–1629.
5. Jackman, J.E., and Alfonzo, J.D. (2013). Transfer RNA modifications: nature's combinatorial chemistry playground. *Wiley Interdiscip. Rev. RNA* 4, 35–48.
6. Boccaletto, P., Machnicka, M.A., Purta, E., Piatkowski, P., Baginski, B., Wirecki, T.K., de Crécy-Lagard, V., Ross, R., Limbach, P.A., Kotter, A., et al. (2018). MODOMICS: a database of RNA modification pathways. 2017 update. *Nucleic Acids Res.* 46 (D1), D303–D307.
7. McKenney, K.M., and Alfonzo, J.D. (2016). From Prebiotics to Probiotics: The Evolution and Functions of tRNA Modifications. *Life (Basel)* 6, E13.
8. El Yacoubi, B., Bailly, M., and de Crécy-Lagard, V. (2012). Biosynthesis and function of posttranscriptional modifications of transfer RNAs. *Annu. Rev. Genet.* 46, 69–95.
9. Suzuki, T. (2021). The expanding world of tRNA modifications and their disease relevance. *Nat. Rev. Mol. Cell Biol.* 22, 375–392.
10. Torres, A.G., Batlle, E., and Ribas de Pouplana, L. (2014). Role of tRNA modifications in human diseases. *Trends Mol. Med.* 20, 306–314.
11. Pavon-Eternod, M., Gomes, S., Geslain, R., Dai, Q., Rosner, M.R., and Pan, T. (2009). tRNA over-expression in breast cancer and functional consequences. *Nucleic Acids Res.* 37, 7268–7280.
12. Goodarzi, H., Nguyen, H.C.B., Zhang, S., Dill, B.D., Molina, H., and Tavazoie, S.F. (2016). Modulated Expression of Specific tRNAs Drives Gene Expression and Cancer Progression. *Cell* 165, 1416–1427.
13. Begley, U., Sosa, M.S., Avivar-Valderas, A., Patil, A., Endres, L., Estrada, Y., Chan, C.T., Su, D., Dedon, P.C., Aguirre-Ghisso, J.A., and Begley, T. (2013). A human

- tRNA methyltransferase 9-like protein prevents tumour growth by regulating LIN9 and HIF1- $\alpha$ . *EMBO Mol. Med.* 5, 366–383.
14. Liu, F., Clark, W., Luo, G., Wang, X., Fu, Y., Wei, J., Wang, X., Hao, Z., Dai, Q., Zheng, G., et al. (2016). ALKBH1-Mediated tRNA Demethylation Regulates Translation. *Cell* 167, 816–828.e16.
  15. Alexandrov, A., Martzen, M.R., and Phizicky, E.M. (2002). Two proteins that form a complex are required for 7-methylguanosine modification of yeast tRNA. *RNA* 8, 1253–1266.
  16. Lin, S., Liu, Q., Lelyveld, V.S., Choe, J., Szostak, J.W., and Gregory, R.I. (2018). Mettl1/Wdr4-Mediated m<sup>7</sup>G tRNA Methylome Is Required for Normal mRNA Translation and Embryonic Stem Cell Self-Renewal and Differentiation. *Mol. Cell* 71, 244–255.e5.
  17. Okamoto, M., Fujiwara, M., Hori, M., Okada, K., Yazama, F., Konishi, H., Xiao, Y., Qi, G., Shimamoto, F., Ota, T., et al. (2014). tRNA modifying enzymes, NSUN2 and METTL1, determine sensitivity to 5-fluorouracil in HeLa cells. *PLoS Genet.* 10, e1004639.
  18. Trimouille, A., Lasseaux, E., Barat, P., Deiller, C., Drunat, S., Rooryck, C., Arveiler, B., and Lacombe, D. (2018). Further delineation of the phenotype caused by biallelic variants in the WDR4 gene. *Clin. Genet.* 93, 374–377.
  19. Shaheen, R., Abdel-Salam, G.M., Guy, M.P., Alomar, R., Abdel-Hamid, M.S., Afifi, H.H., Ismail, S.I., Emam, B.A., Phizicky, E.M., and Alkuraya, F.S. (2015). Mutation in WDR4 impairs tRNA m(7)G46 methylation and causes a distinct form of microcephalic primordial dwarfism. *Genome Biol.* 16, 210.
  20. Braun, D.A., Shril, S., Sinha, A., Schneider, R., Tan, W., Ashraf, S., Hermle, T., Jobst-Schwan, T., Widmeier, E., Majmundar, A.J., et al. (2018). Mutations in WDR4 as a new cause of Galloway-Mowat syndrome. *Am. J. Med. Genet. A.* 176, 2460–2465.
  21. Chen, X., Gao, Y., Yang, L., Wu, B., Dong, X., Liu, B., Lu, Y., Zhou, W., and Wang, H. (2018). Speech and language delay in a patient with WDR4 mutations. *Eur. J. Med. Genet.* 61, 468–472.
  22. Deng, Y., Zhou, Z., Ji, W., Lin, S., and Wang, M. (2020). METTL1-mediated m<sup>7</sup>G methylation maintains pluripotency in human stem cells and limits mesoderm differentiation and vascular development. *Stem Cell Res. Ther.* 11, 306.
  23. Alexandrov, A., Grayhack, E.J., and Phizicky, E.M. (2005). tRNA m<sup>7</sup>G methyltransferase Trm8p/Trm82p: evidence linking activity to a growth phenotype and implicating Trm82p in maintaining levels of active Trm8p. *RNA* 11, 821–830.
  24. Miano, V., Codino, A., Pandolfini, L., and Barbieri, I. (2021). The non-coding epitranscriptome in cancer. *Brief. Funct. Genomics* 20, 94–105.
  25. Chujo, T., and Tomizawa, K. (2021). Human transfer RNA modopathies: diseases caused by aberrations in transfer RNA modifications. *FEBS J.* Published online January 29, 2021. <https://doi.org/10.1111/febs.15736>.
  26. Endres, L., Fasullo, M., and Rose, R. (2019). tRNA modification and cancer: potential for therapeutic prevention and intervention. *Future Med. Chem.* 11, 885–900.
  27. Tian, Q.H., Zhang, M.F., Zeng, J.S., Luo, R.G., Wen, Y., Chen, J., Gan, L.G., and Xiong, J.P. (2019). METTL1 overexpression is correlated with poor prognosis and promotes hepatocellular carcinoma via PTEN. *J. Mol. Med. (Berl.)* 97, 1535–1545.
  28. Wang, C., Wang, W., Han, X., Du, L., Li, A., and Huang, G. (2021). Methyltransferase-like 1 regulates lung adenocarcinoma A549 cell proliferation and autophagy via the AKT/mTORC1 signaling pathway. *Oncol. Lett.* 21, 330.
  29. Hanson, G., and Collier, J. (2018). Codon optimality, bias and usage in translation and mRNA decay. *Nat. Rev. Mol. Cell Biol.* 19, 20–30.
  30. Hia, F., and Takeuchi, O. (2021). The effects of codon bias and optimality on mRNA and protein regulation. *Cell. Mol. Life Sci.* 78, 1909–1928.
  31. Wang, T., Cui, Y., Jin, J., Guo, J., Wang, G., Yin, X., He, Q.Y., and Zhang, G. (2013). Translating mRNAs strongly correlate to proteins in a multivariate manner and their translation ratios are phenotype specific. *Nucleic Acids Res.* 41, 4743–4754.
  32. Lin, S., Liu, Q., Jiang, Y.Z., and Gregory, R.I. (2019). Nucleotide resolution profiling of m<sup>7</sup>G tRNA modification by TRAC-Seq. *Nat. Protoc.* 14, 3220–3242.
  33. Cozen, A.E., Quartley, E., Holmes, A.D., Hrabeta-Robinson, E., Phizicky, E.M., and Lowe, T.M. (2015). ARM-seq: AlkB-facilitated RNA methylation sequencing reveals a complex landscape of modified tRNA fragments. *Nat. Methods* 12, 879–884.

**Supplemental Information**

**METTL1/WDR4-mediated m<sup>7</sup>G tRNA**

**modifications and m<sup>7</sup>G codon usage promote mRNA**

**translation and lung cancer progression**

**Jieyi Ma, Hui Han, Ying Huang, Chunlong Yang, Siyi Zheng, Tiancai Cai, Jiong Bi, Xiaohui Huang, Ruiming Liu, Libin Huang, Yifeng Luo, Wen Li, and Shuibin Lin**

**Supplemental information**  
**Supplemental figures and legends**

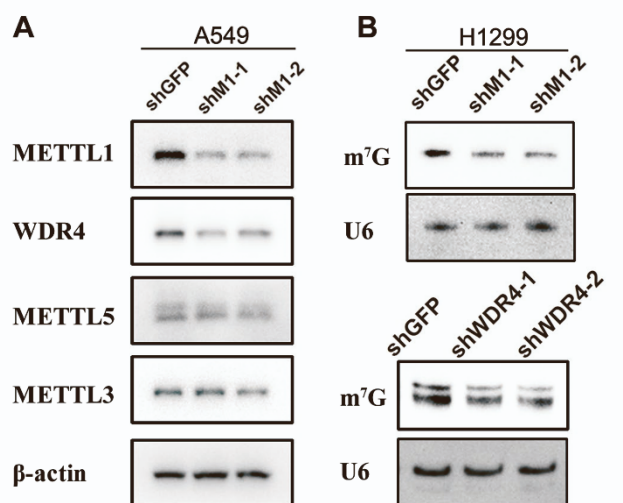


**Figure S1.** (A) Knockdown of METTL1 reduces the expression of WDR4 but not other methyltransferases including METTL3 and METTL5. (B) Knockdown of METTL1 or WDR4 reduced the m<sup>7</sup>G modification of tRNAs in H1299 cells.

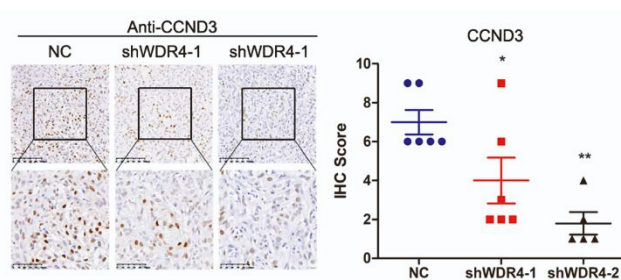


**Figure S2.** IHC confirmed the decreased expression of the identified TE down gene CCND3 in WDR4 depleted xenograft tumors sections. (One-way ANOVA, Student's t test, \* p < 0.05, \*\*\* p < 0.001, compared to shGFP group).

**Table S1.** Oligonucleotides sequences

<b>siRNA and shRNA</b>	
shMETTL1-1	AAATGAGTGCACATCCAGTCG
shMETTL1-2	TTTCTTATCCTTTGGGTCATC
shWDR4-1	AAGAGGCTGTCATCATCACTG
shWDR4-2	TCTAACAGCATAGACAGGTGC
siMETTL1-1	GATGACCCAAAGGATAAGAAA
siMETTL1-2	GGACATCTAGGCACCTCAA
<b>Primers for Real-time qRT-PCR</b>	
β-actin primer	Forward: TTCTACAATGAGCTGCGTGTG Reverse: GGGGTGTTGAAGGTCTCAA
CCND3 primer	Forward: CCTGGGGGCTCTCATGTTTT Reverse: AGGGGCTCCAAAGTACTGA
CCNE1 primer	Forward: ACTCAACGTGCAAGCCTCG Reverse: GCTCAAGAAAGTGCTGATCCC
<b>Northern blot probes</b>	
tRNA-Pro-AGG	CTCGTCCGGGATTTGAACCC
tRNA-Val-AAC	TGTTTCCGCCCGTTTCGAA
tRNA-GlnCTG	CAGAGTGCTAACCATTACACCATGGAACC
U6 snoRNA	TGGAACGCTTCACGAATTTG



**Table S2. RNC seq-TE down gene list**

**Table S3. RNC seq-TE up gene list**

**Table S4. RNC mRNA seq**